Sound speed spatial and temporal variability in Campos and Santos Basins and its influence on traveltime

Pedro Lins de Souza*, Antonio Fernando Härter Fetter Filho & Francisco Carlos Lajús Junior

Universidade Federal de Santa Catarina – UFSC

Abstract

Sound speed (SS) variability in the oceans, if not taken into account, can negatively impact seismic imaging, especially in ultradeep locations (>2000m) such as the hydrocarbon reserves in the Campos and Santos Basins pre-salt region. The current work describes the variability of sound speed on the basins area derived from three reanalysis products: Oras-ECMWF, GLORYS12V1 and Hycom Gofs 3.0. The impact of SS variability on the oceanic region of Santos Basin was also addressed. The model data evaluation with *in situ* ARGO profiles indicated smaller prediction errors on GLORYS results. The sound speed variability was investigated with EOF analysis that revealed a small positive linear trend for central and intermediate layer for ORAS and GLORYS and a spatial pattern of north-south dipole on the second mode. On the oceanic region of Santos Basin the reanalysis profiles agreed reasonably well and presented negative and positive anomalies at interannual scales that caused deviations in traveltime up to $10^{-3}s$.

Introduction

Located in the Western South Atlantic off the coast of southwestern Brazil, the Campos and Santos basins comprise a region of great economic importance due to the presence of some of the world's largest hydrocarbon production fields and reserves (ZHANG et al., 2019). Since the discovery of ultra deep oil fields inside the pre-salt region, there has been an increase of investigation efforts of the underlying basins' geology focusing on seismic reflective methods. Previous studies have found that oversimplifying ocean sound speed models and not taking into account the temporal variability, especially in 4D seismic data sets, leads to significant amplitude and structural errors in seismic imaging (MACKAY et al., 2003). It is also expected that imprecisions in the water column velocity model above ultra deep fields (>2000m) will have a greater impact than in shallower water fields counterparts.

Sound speed in the oceans is empirically related to temperature, pressure and salinity and an increase in any of those properties also increases sound speed. Therefore, sound speed varies in space and time due to differences in water masses composition, due to long term trends, seasonal cycles and dynamic features such as currents, fronts and eddies (JENSEN et al., 2011). The Brazil Current (BC), the western boundary current of the South Atlantic's subtropical gyre is the main dynamic feature in the study area's surface circulation. Its flow is associated with the warm and saline Tropical Water (TW) and the South Atlantic Central Water (SACW) south of 22°S (CIRANO et al., 2006).

The SACW, the South Atlantic's subtropical gyre thermocline water, is transported to the BC by the Southern South Equatorial Current (SSEC) that encounters the western boundary at depth-dependent latitudes (STRAMMA and ENGLAND, 1999). At intermediate depths, the SSEC is mainly zonally oriented (SCHMID, 2014) and reaches the western boundary at 30°S and is associated with the Antarctic Intermediate Water (AAIW, STRAMMA and ENGLAND, 1999). This zonal flow at 30°S was also observed in shallower water circulation (VIANNA and MENEZES, 2011; SCHMID, 2014) and has also been described as part of the double cell representation of the subtropical gyre (VIANNA and MENEZES, 2011). Both basins are subject to intense mesoscale variability due to the shedding of CB eddies that can reach deep waters in the oceanic region (ANDRIONI et al., 2013) and westward propagating eddies generated near the Agulhas retroflection that can cause deviations from the mean thermohaline profiles reaching depths greater than 800m (GUERRA et al., 2018).

Even though the South Atlantic's thermohaline variability has been addressed in several studies covering decadal and multi-decadal warming trends (ROEMMICH et al., 2015; SCHMIDTKO and JOHNSON, 2012; GIGLIO and JOHNSON, 2017) and warming and salinization related to the increase of the Agulhas Leakage (BIASTOCH et al., 2008), comparatively fewer studies have focused on the Santos and Campos basins ocean acoustic environment. CODATO et al. (2012) and CALADO et al. (2008) have applied a numeric ocean model to the prediction of sound speed and acoustic propagation on focused on the coastal resurgence of Cabo Frio. More research is still needed to characterize the acoustic environment and sound propagation along the whole extension of the basins, especially at ultradeep locations.

Therefore, this study aimed to investigate the sound speed variability across the Campos and Santos Basins and the evolution of the sound speed profile (SSP) and traveltime at the oceanic region of Santos Basin using sound speed obtained from temperature and salinity data from three global ocean reanalysis.

Methods

Reanalysis models

Temperature and salinity data sets from three global ocean reanalysis were used to compute monthly mean fields of sound speed for the study region. The basic configuration of the reanalysis products and time coverage are presented in Table

Table 1: Global ocean reanalysis settings and time coverage considered.

	ORAS5-ECMWF	GLORYS12V1	HYCOM Gofs 3.0
Numerical model	Nemo 3	Nemo 3	Hycom
Atmospheric forcing	ECMWF ERA-Interim	ECMWF ERA-Interim	CFSR-NCEP
Horizontal resolution	¼°	1/12°	1/12°
N° of vertical levels	75	50	50
Time coverage	1979 - 2018	1992-2018	1993-2012

1. The Ocean Reanalysis System 5 (ORAS5, furthermore referred to as ORAS) has the longest time coverage (1979-2018), the finer vertical resolution of 75 vertical levels and the coarser horizontal resolution of ¼° from all the models considered (ZUO et al., 2018). The second data product was the GLORYS12V1 (furthermore referred to as GLORYS) that covers the ARGO era (1992-2021, FERRY et al., 2010) and shares some similarities with ORAS such as the underlying numerical model (NEMO 3), an ORCA numerical grid type and atmospheric forcing (ECMWF - Era Interim, FERNANDEZ and LELLOUCHE, 2018; ZUO et al., 2018). The HYCOM Gofs 3.0 (furthermore referred to as HYCOM) was the third reanalysis considered and differs from the other two reanalysis in the underlying numerical model (HYCOM) and atmospheric forcing from the Climate Forecast System Reanalysis (CFSR-NCEP).

Sound speed calculations

All sound speed and related calculations were performed with the Gibbs Seawater Toolbox routines that use the computationally efficient 75-term polynomial approximation to the International Thermodynamic Equation of Seawater 2010 (TEOS-10, ROQUET et al., 2015) on temperature and salinity fields from the reanalysis data products and *in situ* thermohaline profiles.

EOF analysis of the sound speed content on water masses layers

To analyze sound speed variability patterns along Campos and Santos basins, each models' sound speed fields were depth-averaged to generate representative time series for the water masses in the study site. The interface depths between the water masses were defined by σ_0 levels following PEREIRA et al. (2014) that establishes $25.7kg \cdot m^{-3}$ as the TW-SACW interface, $26.8kg \cdot m^{-3}$ for the SACW-AAIW interface and $27.5kg \cdot m^{-3}$ for the AAIW-NADW interface. Variability modes were obtained through empirical orthogonal functions (EOF) on the detrended and deseasoned sound speed series. The eigenvectors (spatial patterns) are presented as correlation to the principal components (PCs) time series, also provided for each mode (HANNACHI et al., 2007).

Acoustic traveltime

To access the impact of sound speed variability on acoustic waves propagation, first-arrival traveltime was computed for the sound speed profiles with the integral solution to the eikonal equation in ray coordinates

$$\tau = \int_{\Gamma} \frac{1}{c} dl, \tag{1}$$

where τ is the traveltime, $1/c$ is the slowness and Γ is the ray trajectory, considered simply as straight ray across the water column and l is the distance along the ray (JENSEN et al., 2011).

Models evaluation

The models' performance in representing sound speed profiles was evaluated against SSPs obtained from measured termohaline profiles from the ARGO drifters Project. The profiles were linearly interpolated from the reanalysis data at ARGO profile locations, converted to SSP and for each location the 95th percentile errors were estimated from the module of the difference between profiles (Figure 1).

Higher 95th percentile errors occurred near the continental slope possibly reflecting the models' poor ocean representation at steep slopes. All models also indicated a region of higher than usual error near $23°S\ 41°W$ that may be related to mesoscale variability including the semi-permanent Cabo de São Tomé Eddie near that region. GLORYS SSPs accounted for lower errors compared to the other models which varied from $0ms^{-1}$ to $5ms^{-1}$ on most of the domain and consistently exhibited errors bellow $2ms^{-1}$ in the deeper part of the Campos and Santos Basins. Comparatively, in only a few profile locations the percentile errors were lower than $4ms^{-1}$ for HYCOM results although few comparisons could be made due to the HYCOM's shorter simulation period (covering from 1993 to 2012).

Results and Discussion

In order to investigate the sound speed variability, EOFs were computed from the sound speed time series in each water mass layer. The spatial patterns and correspondent principal components (PCs) are presented in Figure 2, 3 and 4. The NADW layer analysis was omitted due to lower variability. Only the first two EOFs are considered. The first mode for all analysis (along all water masses and models) displayed loadings of the same signal across the domain and percentage variances above 40%, except for the HYCOM results in the SACW (13%) and AAIW (15%) layer, a indicative that the physical forcing that most impact sound speed variability actuate on a wider area inside the South Atlantic. Other recurring pattern found included a north-south dipole with an axis at 25° S-26° S which was frequently found as the second mode of variability, although the GLORYS EOF 2 pattern in the AAIW resembles an east-west dipole. Between the TW and SACW layers the axis of the dipole moves slightly to the north.

The north-south dipole may be related to the advection of thermohaline properties to the study site from the west. Visualizations of the evolution of sound speed fields (not shown) indicate that sound speed anomalies enter the study area zonally south of 25°S. Previous ocean circulation studies corroborates zonal east-west flow in that latitudinal band from the upper layers to the intermediate water depth ($\sim 1000m$, BOEBEL et al., 1997; VIANNA and MENEZES, 2011). This flow is maintained in intermediate water depths by the southern limb of the SEC, that encounters the Santos Basin at 26°S-28°S and bifurcates in the north/south direction.

The Principal Compenents (PCs) series for the TW layer

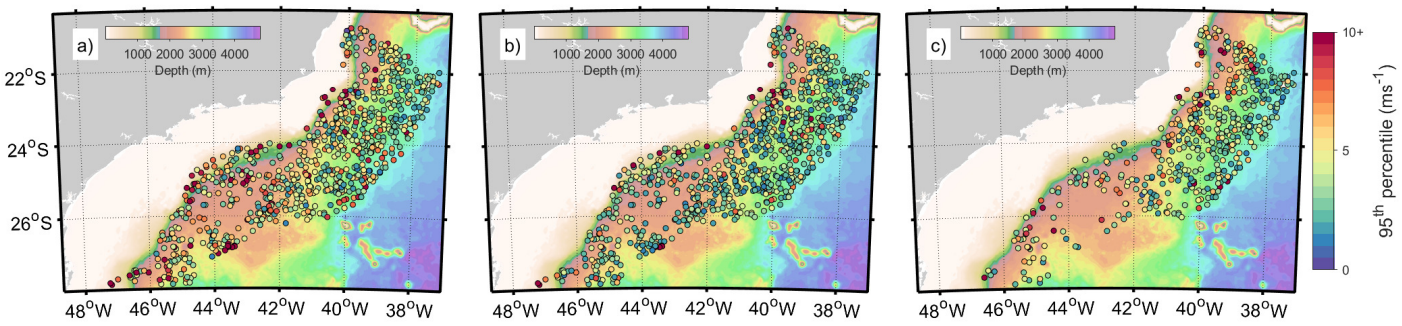

Figure 1: 95th percentile of the error bias between SSPs estimated from ARGO profiles within Campos and Santos basins and profiles interpolated from ORAS (a), GLORYS (b) and HYCOM (c) fields.

across all models displayed high frequency variability, which was attenuated in the layers bellow the surface. The PC2 for the TW layer also displays interannual variability with periods of 4 to 10 years, possibly related to South Atlantic's sea surface temperature (SST) variability modes caused by shifts in the Subtropical High (VENEGAS et al., 1996). The SACW and AAIW layer for each model had similar PC time series and presented positive linear trends for the ORAS and GLORYS models, possibly related to the warming of the South Atlantic's subtropical gyre (ROEMMICH et al., 2015) and intermediate waters (SCHMIDTKO and JOHNSON, 2012; GIGLIO and JOHNSON, 2017). Contrarily, HYCOM's PCs had a small negative trend. The disparity from the other models may be attributed to HYCOM's shorter time series considered (see Figure 5, the years after 2012 had positive sound speed anomalies).

The sound speed profile variability through time in the oceanic region of Santos Basin (25.54°S 42.81°W) is represented in Figure 5 as anomalies from the mean sound speed profile. Also provided are the time series of traveltime, indicating the phase shift that an acoustic wave undergoes while propagating from the bottom to the surface through the SSPs. The contours from all three models agree at long term patterns and corroborates the linear trends found in the EOF analysis for the SACW and AAIW layers and ORAS and GLORYS models displaying a shift from negative to positive anomalies through time.

GLORYS results accounts for the most noticeable anomalies in module, which also reaches greater depths beyond the inferior limits of the AAIW (indicated by the 27.5σ isoline in Figure 5). ORAS results displayed less variability at both rate and magnitude due to the eddy-permitting resolution (¼°) in contrast to the eddy-resolving (1/12°) resolution of the other two models, which results in a diminished variance in ORAS traveltime series in comparison to the other models.

A negative anomaly in GLORYS results that lasted from 1997 to 2001 and peaked in the summer of 1999 produced the greatest effect in the associated traveltime series. ORAS and HYCOM results also displayed cold anomalies during 1999 with lesser duration and magnitude. For that effect, HYCOM traveltime series does not display abrupt changes and rather appears to have stable mean and variance. A second period of higher incidence of negative anomalies occurs in GLORYS

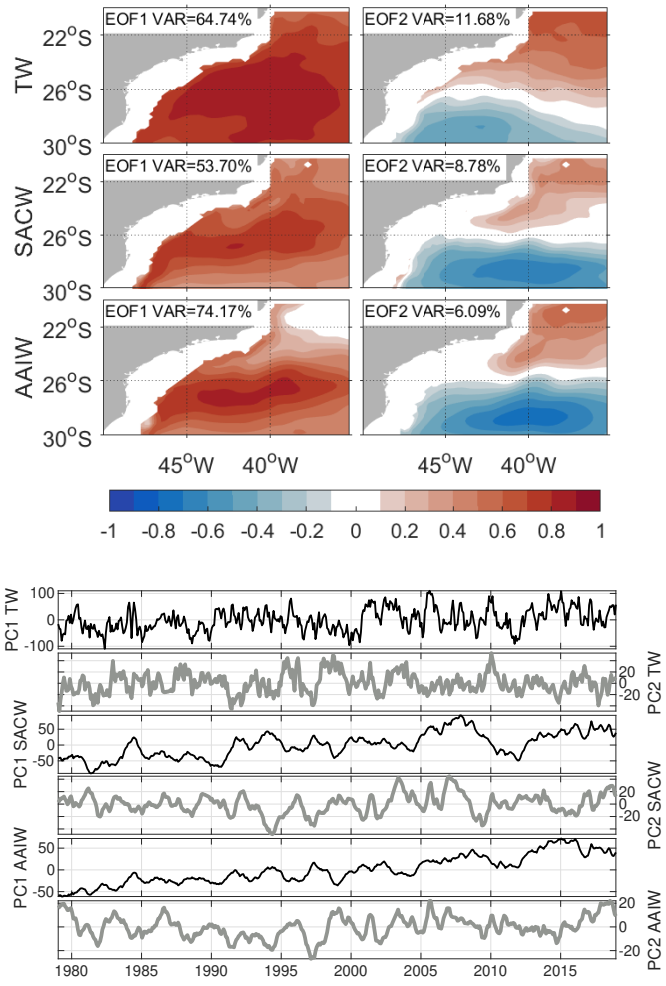

Figure 2: Spatial patterns and corresponding PC time series for the first and second mode of variability (EOF1 and EOF2) obtained from the sound speed series on the TW, SACW and AAIW layers for ORAS model. Spatial patterns are expressed as correlation to the equivalent PC time series. Contour interval is 0.1 with the zero-line omitted. The explained variance of each mode is expressed as percentage on the top panel of each map.

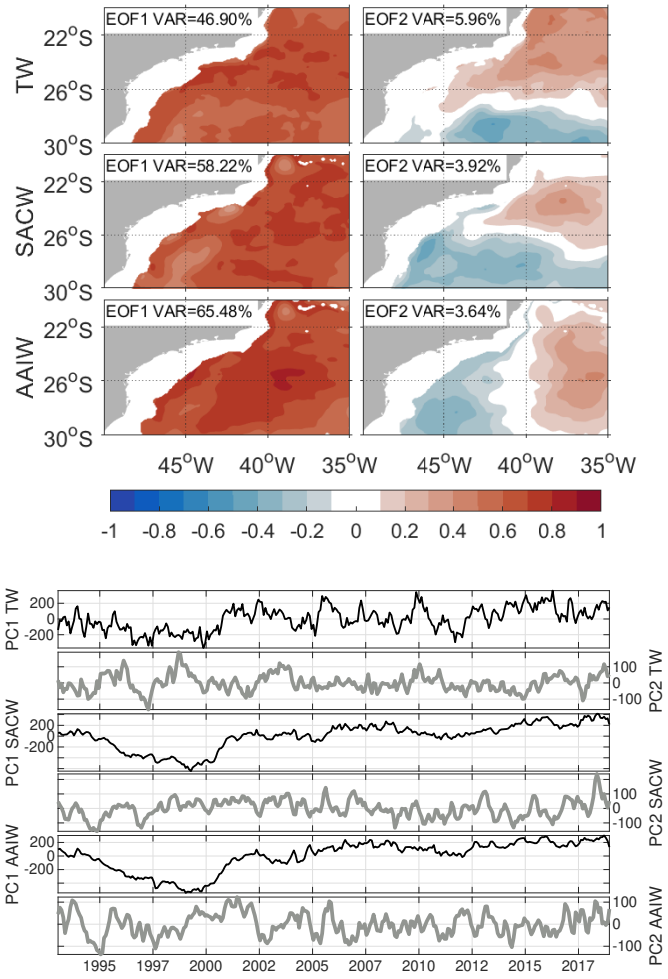

Figure 3: Same as in Figure 2 for the GLORYS model.

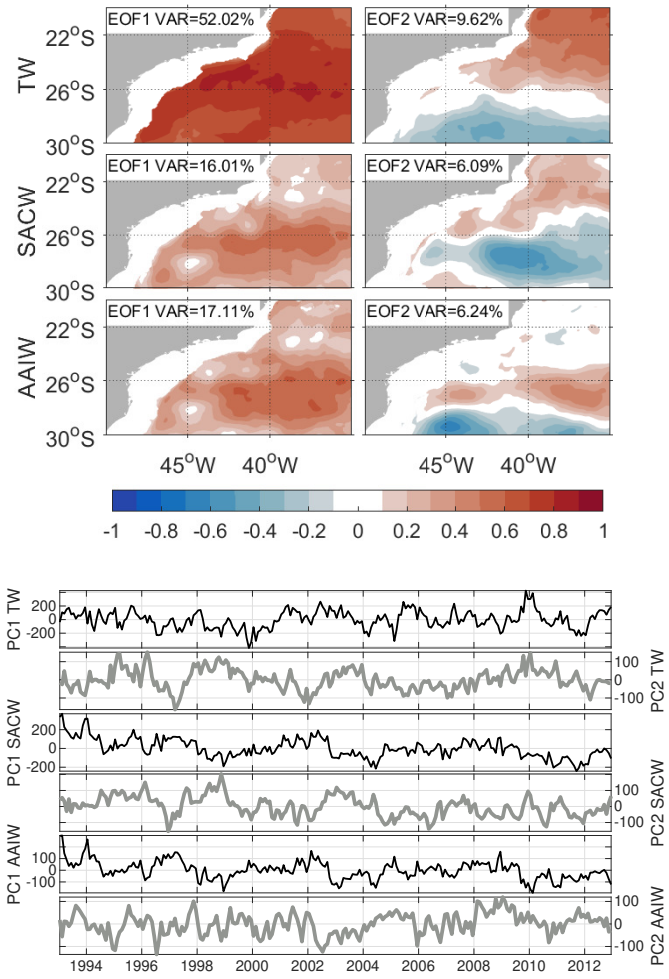

Figure 4: Same as in Figure 2 for the HYCOM model.

results from mid-2010 to 2012 which is corroborated in the other models with similar duration. A period of positive anomalies during from 2007 to 2009 occurs in ORAS results stratified at 200m depth and is partially corroborated by the GLORYS results.

The variability observed may be explained by the lateral advection of thermohaline properties caused by eddy propagation. Eddies detached from the Brazil Current and eddies shed by the Agulhas current retroflection can reach the oceanic part of Santos Basin and change the local thermohaline profile to up to 800m (ANDRIONI et al., 2013; GUERRA et al., 2018).

Summary and Conclusions

The current work presents an application of termohaline data from ocean reanalysis products on the characterization of sound speed spatial and temporal variability across Campos and Santos basins. In the first moment, comparisons with measured *in situ* data were provided, later the sound speed content across both basins was divided by depth layers representative of the local water masses and modes of variability were obtained. Lastly, the time evolution of the sound speed profile in in the oceanic region of Santos Basins was presented accompanied by the variability's effect on traveltime as a proxy of the acoustic environment.

The main results can be summarized as follows:

- The 95th percentile bias analysis applied with ARGO profile data indicated that GLORYS often had smaller prediction errors, although retaining some higher error values near the continental slope
- The SACW and AAIW layers for the ORAS and GLORYS (models with longer time series) presented a positive trend that may be related to long term trends of warming of the subtropical gyre or decadal oscillations of the South Atlantic
- The second mode of sound speed variability across the models and water masses layers often displayed a north-south dipole and may be related to the central and intermediate depths circulation
- Variability in the SACW and AAIW layers cause most of the impact on time series of traveltime
- Interannual periods of positive and negative anomalies at central and intermediate depths are consistent between models and may be explained by the advection of eddies from the CB and westward propagating eddies

Acknowledgements

The authors are grateful to André Bulcão and Bruno Dias for the fruitful backstage discussion. This research was supported by Petrobras through "Determinação da velocidade do som da coluna d'água utilizando dados de levantamentos sísmicos" project with Universidade Federal of Santa Catarina (UFSC), and ANP through the R&D levy regulation, process: 2017/00071-6.

References

ANDRIONI, M.; MOREIRA LIMA, J. A.; GUERRA, L. A.; RIBEIRO, E. O.; PAIVA NUNES, L. M.; CECCOPIERI, W.; DE SOUZA REGO, V., and DE OLIVEIRA, S. M., 2013, Ocean eddies influence on lula field, santos basin, brazil: ASME 2012 31st international conference on ocean, offshore and arctic engineering, 189–193. (tex.organization: American Society of Mechanical Engineers Digital Collection).

BIASTOCH, A.; BÖNING, C. W., and LUTJEHARMS, J. R. E., 2008, Agulhas leakage dynamics affects decadal variability in Atlantic overturning circulation: Nature, **456**, 489–492.

BOEBEL, O.; SCHMID, C., and ZENK, W., 1997, Flow and recirculation of antarctic intermediate water across the rio grande rise: **102**, 20967–20986.

CALADO, L.; GANGOPADHYAY, A., and DA SILVEIRA, I., 2008, Feature-oriented regional modeling and simulations (FORMS) for the western South Atlantic: Southeastern Brazil region: **25**, 48–64.

CIRANO, M.; MATA, M. M.; CAMPOS, E. J., and DEIRÓ, N. F., 2006, A circulação oceânica de larga-escala na região oeste do Atlântico Sul com base no modelo de circulação global OCCAM: Revista Brasileira de Geofísica, **24**, 209–230. (tex.publisher: SciELO Brasil).

CODATO, G.; CALADO, L.; MARTINS, N. E.; WATANABE, W. D.; DOMINGUES, R. M., and JESUS, S. M., 2012, Acoustic prediction using a feature-oriented regional modeling system and acoustic inversion: Proceedings of Meetings on Acoustics, 070052, Acoustical Society of America.

FERNANDEZ, E. and LELLOUCHE, J., 2018, Product user manual for the global ocean physical reanalysis product GLOBAL-REANALYSIS$_p$HYâ01â30: Technical report, EU Copernicus Marine Service.

FERRY, N.; PARENT, L.; GARRIC, G.; BARNIER, B.; JOURDAIN, N. C., and OTHERS, 2010, Mercator global Eddy permitting ocean reanalysis GLORYS1V1: Description and results: Mercator-Ocean Quarterly Newsletter, **36**, 15–27.

GIGLIO, D. and JOHNSON, G. C., 2017, Middepth decadal warming and freshening in the South Atlantic: MIDDEPTH S. ATLANTIC WARMS AND FRESHENS: Journal of Geophysical Research: Oceans, **122**, 973–979.

GUERRA, L. A. A.; PAIVA, A. M., and CHASSIGNET, E. P., 2018, On the translation of Agulhas rings to the western South Atlantic Ocean: Deep Sea Research Part I: Oceanographic Research Papers, **139**, 104–113.

HANNACHI, A.; JOLLIFFE, I. T., and STEPHENSON, D. B., 2007, Empirical orthogonal functions and related techniques in atmospheric science: A review: International Journal of Climatology, **27**, 1119–1152.

JENSEN, F. B.; KUPERMAN, W. A.; PORTER, M. B., and SCHMIDT, H., 2011, Computational ocean acoustics: Springer Science & Business Media.

MACKAY, S.; FRIED, J., and CARVILL, C., 2003, The impact of water-velocity variations on deepwater seismic data: The Leading Edge, **22**, 344–350.

PEREIRA, J.; GABIOUX, M.; MARTA-ALMEIDA, M.; CIRANO, M.; PAIVA, A., and AGUIAR, A., 2014, The bifurcation of the western boundary current system of the South Atlantic Ocean: **32**, 241–257.

ROEMMICH, D.; CHURCH, J.; GILSON, J.; MONSELESAN, D.; SUTTON, P., and WIJFFELS, S., 2015, Unabated planetary warming and its ocean structure since 2006: Nature Climate Change, **5**, 240–245.

ROQUET, F.; MADEC, G.; MCDOUGALL, T. J., and BARKER, P. M., 2015, Accurate polynomial expressions for the density and specific volume of seawater using the TEOS-10 standard: Ocean Modelling, **90**, 29–43.

SCHMID, C., 2014, Mean vertical and horizontal structure of the subtropical circulation in the South Atlantic from three-dimensional observed velocity fields: Deep Sea Research Part I: Oceanographic Research Papers, **91**, 50–71. (Publisher: Elsevier).

SCHMIDTKO, S. and JOHNSON, G. C., 2012, Multidecadal Warming and Shoaling of Antarctic Intermediate Water*: Journal of Climate, **25**, 207–221.

STRAMMA, L. and ENGLAND, M., 1999, On the water masses and mean circulation of the South Atlantic Ocean: Journal of Geophysical Research: Oceans, **104**, 20863–20883.

VENEGAS, S. A.; MYSAK, L. A., and STRAUB, D. N., 1996, Evidence for interannual and interdecadal climate variability in the South Atlantic: Geophysical Research Letters, **23**, 2673–2676.

VIANNA, M. L. and MENEZES, V. V., 2011, Double-celled subtropical gyre in the South Atlantic Ocean: Means, trends, and interannual changes: Journal of Geophysical Research, **116**, C03024.

ZHANG, G.; QU, H.; CHEN, G.; ZHAO, C.; ZHANG, F.; YANG, H.; ZHAO, Z., and MA, M., 2019, Giant discoveries of oil and gas fields in global deepwaters in the past 40 years and the prospect of exploration: Journal of Natural Gas Geoscience, **4**, 1–28. (tex.publisher: Elsevier).

ZUO, H.; BALMASEDA, M.; MOGENSEN, K., and TIETSCHE, S., 2018, OCEAN5: the ECMWF ocean reanalysis system and its real-time analysis component: European Centre for Medium-Range Weather Forecasts.

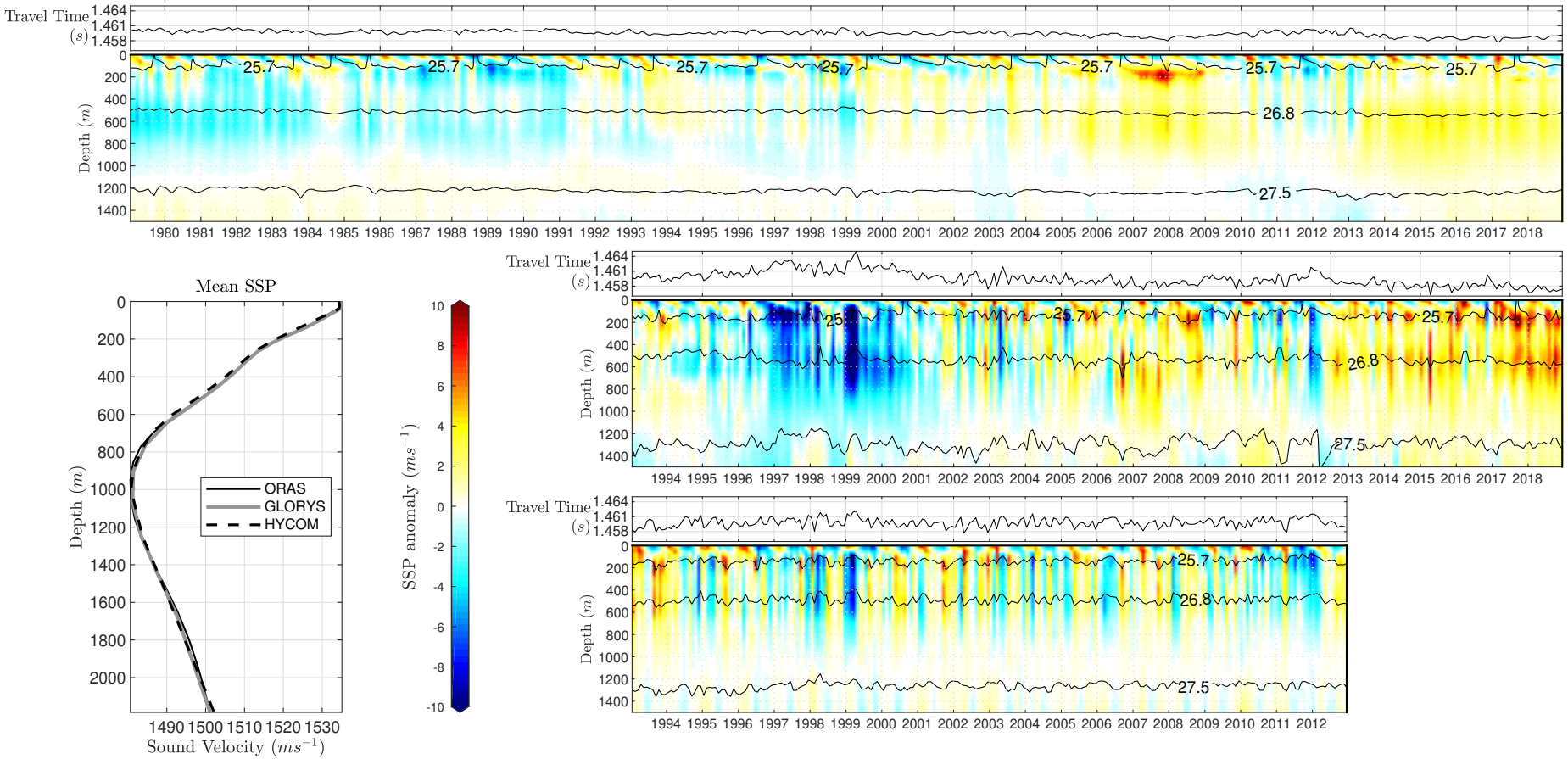

Figure 5: Hovmöller diagrams of sound speed anomaly for the top 1500m and time series of traveltime for ORAS (top), GLORYS (center) and HYCOM (bottom). The SSP mean profiles for each model are also provided. The solid contours indicate the TW-SACW ($\sigma = 25.7 kg \cdot m^{-3}$), SACW-AAIW ($\sigma = 26.8 kg \cdot m^{-3}$) and AAIW-NADW ($\sigma = 27.5 kg \cdot m^{-3}$) interfaces (PEREIRA et al., 2014).